responding chlorides. However, it seems evident from the data of Table I that the bromine transfer rates are substantially higher for a given metal carbonyl radical. This is, of course, consistent with the generally lower C–Br bond energies as compared with those for C–Cl and with the lower polarity of the C–Br bond. It is noteworthy that the rate constant for reaction of $Mn(CO)_5$· with CBr_4 approaches the diffusion-controlled limit. Presumably the process is overall substantially exothermic. The present results provide the first direct and extensive quantitative evaluations of halogen atom transfer rates. They substantiate that under appropriate conditions halogen atom transfer can compete with alternative reaction pathways for the radicals, such as recombination or substitution.[13]

Acknowledgment. We are grateful to S. G. Smith for advice and permission to use his fast stopped-flow apparatus. We are also grateful to J. Wehmer for his assistance in performing the laser experiments.

Registry No. $Mn(CO)_4P(n\text{-}Bu)_3$·, 45264-38-8; $Mn(CO)_4P(o\text{-}i\text{-}Pr)_3$·, 93041-25-9; $Mn(CO)_4P(i\text{-}Bu)_3$·, 92186-52-2; $Mn(CO)_4P(i\text{-}Pr)_3$·, 92186-53-3; $Mn(CO)_4P(C_6H_{11})_3$·, 47560-29-2; $Mn(CO)_3[P(i\text{-}Bu)_3]_2$·, 81971-50-8; $Mn(CO)_3[P(i\text{-}Pr)_3]_2$·, 83634-20-2; $Mn(CO)_3[P(n\text{-}Bu)_3]_2$·, 67551-64-8; $Mn(CO)_5$·, 15651-51-1; CBr_4, 558-13-4; $CHBr_3$, 75-25-2; $C_6H_5CH_2Br$, 28807-97-8; CH_2Br_2, 74-95-3; $CHCl_3$, 67-66-3; $C_6H_5CH_2Cl$, 25168-05-2; CH_2Cl_2, 75-09-2; CCl_4, 56-23-5; Cl_2, 7782-50-5; Br_2, 7726-95-6.

Formation and Chemistry of the Homologous Series of Nitrido Clusters: $[Ru_4N(CO)_{12}]^-$, $[Ru_5N(CO)_{14}]^-$, and $[Ru_6N(CO)_{16}]^-$ †

Margaret L. Blohm[1] and Wayne L. Gladfelter*[2]

Department of Chemistry, University of Minnesota, Minneapolis, Minnesota 55455

Received July 3, 1984

The reaction of coordinated isocyanate ligands to give new nitrido clusters is explored. The thermolysis of $[Ru_4(NCO)(CO)_{13}]^-$ gives $[Ru_4N(CO)_{12}]^-$ in 78% recrystallized yield after 24 h. When the trinuclear isocyanate clusters $[Ru_3(NCO)(CO)_{10}]^-$ and $[Ru_3(NCO)(CO)_{11}]^-$ are heated with 1 equiv of $Ru_3(CO)_{12}$, the hexanuclear nitrido cluster $[Ru_6N(CO)_{16}]^-$ can be isolated in 82% yield. $[Ru_6N(CO)_{16}]^-$ reacts rapidly with CO at room temperature to give $[Ru_5N(CO)_{14}]^-$ in quantitative yield. A single-crystal X-ray crystallographic study of $(PhCH_2Et_3N)[Ru_5N(CO)_{14}]$ [$P\bar{1}$ space group, a = 12.123 (6) Å, b = 14.263 (5) Å, c = 10.642 (3) Å, α = 104.74 (3)°, β = 93.28 (3)°, γ = 80.25 (4)°, Z = 2] revealed a square-based pyramid of metal atoms with the nitrogen positioned slightly below the square face. Other interconversions among the nitrido clusters are also discussed. At high CO pressure, the isocyanate ligand can be reformed from the nitrido clusters.

Introduction

The source of nitrogen in almost all the known nitrido clusters is one form or another of nitric oxide. Practically, nitrosonium ion and preformed metal nitrosyl complexes are used to form nitrido clusters.[3] The only cluster that does not make use of NO is $[Ru_6N(CO)_{16}]^-$, as reported in the preliminary communication of this work.[4] In this case, isocyanate is the species donating the nitrogen atom. One of the reasons we are interested in these nitrido clusters is to establish a relationship with the structures and reactivity of surface-coordinated nitrogen atoms. These latter species are invoked as intermediates in many important catalytic reactions such as the Haber process[5] and the reduction of NO_x pollutants.[6]

One of the interesting features of metals that catalyze eq 1 is the appearance of isocyanates on the metal surface

$$2NO + CO \rightarrow N_2O + CO_2 \quad (1)$$

during the catalytic reaction.[7] It has been suggested that the isocyanate arises by eq 2, which must obviously be

$$N(ads) + CO(ads) \rightleftharpoons NCO(ads) \quad (2)$$

reversible for the catalyst to be active. Other workers[8] have capitalized on this reaction as a means of forming a new N–C bond by adding H_2 to the mixture of NO and CO. The end result (eq 3) is the catalytic synthesis of isocyanic acid.

$$NO + 2CO + {}^1/_2H_2 \rightarrow HNCO + CO_2 \quad (3)$$

As mentioned above this paper discusses the conversion of NCO^- coordinated to clusters into nitrido clusters. Besides generating three new nitrido clusters, the reactions bear a similarity to the surface chemistry.

Experimental Section

PPN(Cl)[9] (PPN = bis(triphenylphosphine)nitrogen(1+)), PPN(N_3),[10] PPN(NCO),[10] $Ru_3(CO)_{12}$,[11] PPN[Ru_4(NCO)$(CO)_{13}$],[12] $(PPN)_2[Ru_6(CO)_{18}]$,[13] and PPN[$Ru(CO)_3(NO)$][14] were prepared according to published procedures. Tetrahydrofuran (THF) and

† Dedicated to the memory of Professor Earl L. Muetterties.

(1) NSF Predoctoral Fellow, 1982–1985.
(2) Alfred P. Sloan Fellow, 1983–1985.
(3) Gladfelter, W. L. *Adv. Organomet. Chem.*, in press.
(4) Blohm, M. L.; Fjare, D. E.; Gladfelter, W. L. *Inorg. Chem.* **1983**, *22*, 1004–1006.
(5) Osaki, A.; Aika, K. *Catal. Sci. Technol.* **1981**, *1*, 87.
(6) Eisenberg, R.; Hendriksen, D. E. *Adv. Catal.* **1979**, *28*, 79–172.
(7) Unland, M. L. *J. Phys. Chem.* **1973**, *77*, 1952–1956.
(8) Voorhoeve, R. J. H.; Trimble, L. E. *J. Catal.* **1978**, *54*, 269–280.
(9) Ruff, J. K.; Schlentz, W. J. *Inorg. Synth.* **1974**, *15*, 85–87.
(10) Martinsen, A.; Songstad, J. *Acta Chem. Scand., Ser. A* **1977**, *A31*, 645–650.
(11) Mantovani, A.; Cenini, S. *Inorg. Synth.* **1976**, *16*, 47–48.
(12) Fjare, D. E.; Jensen, J. A.; Gladfelter, W. L. *Inorg. Chem.* **1983**, *22*, 1774–1780.
(13) Eady, C. R.; Jackson, P. F.; Johnson, B. F. G.; Lewis, J.; Malatesta, M. C.; McPartlin, M.; Nelson, W. J. H. *J. Chem. Soc., Dalton Trans.* **1980**, *383*–392.
(14) Stevens, R. E.; Fjare, D. E.; Blohm, M. L.; Gladfelter, W. L., Paper 153, 17th Great Lakes Regional Meeting of the American Chemical Society, St. Paul, MN, June 1983; American Chemical Society: Washington, DC, 1983.

0276-7333/85/2304-0045$01.50/0

Table I. Spectroscopic Data

cluster	color	^{15}N, ppm (CH_2Cl_2)	ν_{CO}, cm^{-1} (THF)
$PPN[Ru_6N(CO)_{16}]$	brick red	559.8	2010 vs, 1960 sh, 1839 m
$PPN[Ru_5N(CO)_{14}]$	red	464.9	2060 w, 2013 vs, 1999 s, 1960 m, 1820 m
$PPN[Ru_4N(CO)_{12}]$	orange	519.1	2066 w, 2032 s, 2000 vs, 1975 sh, 1941 w

diethyl ether were distilled from sodium benzophenone ketyl under nitrogen. Hexane was dried by distillation from sodium metal under nitrogen. Methylene chloride was distilled from P_2O_5 immediately prior to use. All reactions were carried out under an N_2 atmosphere. Infrared spectra were recorded on a Beckman Model No. 4250 spectrophotometer, and NMR data were recorded on a Nicolet NTCFT-1130 300-MHz spectrophotometer. Enriched (50%) $PPN[Ru_6{}^{15}N(CO)_{16}]$ and $PPN[Ru_5{}^{15}N(CO)_{14}]$ for the ^{15}N NMR experiments were prepared from 99% enriched $Na^{15}N{=}N{=}N$ obtained from Stohler Isotope Chemicals. $PPN[Ru_4{}^{15}N(CO)_{12}]$ was prepared by using 95% enriched $Na^{15}NO_2$ purchased from Merck, Sharp and Dohme. Each ^{15}N and ^{13}C NMR experiment was conducted with CH_2Cl_2 as the solvent (3.0 mL) in a 12-mm tube with $Cr(acac)_3$ (53 mg) added as the shiftless relaxation reagent. Nitromethane was used as an external reference, set at 379.60 ppm downfield from NH_3 (liquid, 25 °C),[15] and all data are reported relative to NH_3. The ^{13}C data are reported relative to Me_4Si. The $KN^{13}CO$ was purchased from Stohler Isotope Chemicals and found to be 62% enriched with ^{13}C. The spectroscopic data for the new compounds are summarized in Table I. The equipment used to study the high-pressure reactions is described elsewhere.[16]

Preparation of $PPN[Ru_6N(CO)_{16}]$. A. A 50-mL three-neck round-bottom flask was equipped with a reflux condenser fit with gas adapter leading to a Nujol bubbler, a serum cap, and a gas adapter and was charged with 100.0 mg (0.156 mmol) of $Ru_3(CO)_{12}$ and 45.4 mg (0.0782 mmol) of $PPN(N_3)$. A 15-mL sample of THF was added by syringe, and vigorous evolution of gas accompanied a color change from orange to red. The solution was stirred at room temperature until all $PPN(N_3)$ was dissolved (10 min) and then was lowered into an 80 °C oil bath. The solution became red-brown after 15 min and was refluxed for 12 h. The THF was evaporated, leaving a red-brown oil, which was extracted with 3 × 10 mL of diethyl ether and filtered. The deep red filtrate was reduced in volume to 20 mL, to which 20 mL of hexane was added. Rapid mixing led to the isolation of 102 mg of brick red microcrystals (82%). The product was recrystallized from diethyl ether/hexane. Anal. Calcd for $PPN[Ru_6N(CO)_{16}]$: C, 38.86; H, 1.88; N, 1.74. Found: C, 38.68; H, 2.00; N, 1.63.

B. $(PPN)_2[Ru_6(CO)_{18}] + NOPF_6$. A 15-mL sample of CH_2Cl_2 was vacuum distilled into a Schlenk tube containing $(PPN)_2[Ru_6(CO)_{18}]$ (18.8 mg, 0.0086 mmol) and $NOPF_6$ (1.5 mg, 0.0086 mmol) that was cooled with liquid N_2. The red-brown solution was warmed to room temperature. After the solution was stirred for 12 h, the CH_2Cl_2 was removed under vacuum and the remaining brick red residue extracted with Et_2O. The Et_2O solution was filtered, and the volume was reduced to 3 mL. The filtrate was layered with 5 mL of hexane, yielding 5.2 mg of brick red microcrystalline $PPN[Ru_6N(CO)_{16}]$ (38%).

Synthesis of $PPN[Ru_4(N^{13}CO)(CO)_{13}]$. A 10-mL sample of THF was added to a Schlenk tube containing $Ru_3(CO)_{12}$ (20.0 mg, 0.047 mmol) and $PPN(N^{13}CO)$ (27.2 mg, 0.047 mmol). The solution was stirred until all of the $PPN(N^{13}CO)$ was consumed (1 h). After the solvent was removed under vacuum, the dark red residue was extracted with Et_2O, filtered, reduced in volume to 10 mL, and layered with 15 mL of hexane. After 2 days, this gave 32 mg of purple, slightly air-sensitive crystals (68% yield). The ν_{NCO} absorbances for the ^{13}C isocyanates appeared at 2170 cm^{-1} for $[Ru_3(N^{13}CO)(CO)_{11}]^-$, 2148 cm^{-1} for $[Ru_3(N^{13}CO)(CO)_{10}]^-$, and 2131 cm^{-1} for $[Ru_4(N^{13}CO)(CO)_{13}]^-$.

Preparation of $PPN[Ru_5N(CO)_{14}]$. $PPN[Ru_6N(CO)_{16}]$ (50.0 mg, 0.031 mmol) was dissolved in 10 mL of THF. CO was gently bubbled through the deep red solution for 15 min causing the color to become a bright orange-red. The solvent was evaporated, and the resulting oil was washed with 3 × 10 mL of hexane. The remaining hexane insoluble oil was extracted with 2 × 10 mL of diethyl ether, filtered, and reduced in volume to 5 mL. Adding 5 mL of hexane to the rapidly stirring filtrate gave 42.8 mg of $PPN[Ru_5N(CO)_{14}]$ (95%). Anal. Calcd for $PPN[Ru_5N(CO)_{14}]$: C, 41.41; H, 2.08; N, 1.93. Found: C, 41.38; H, 2.17; N, 1.91.

Preparation of $PPN[Ru_4N(CO)_{12}]$. A. $PPN[Ru_4(NCO)(CO)_{13}]$ (190 mg, 0.141 mmol) was dissolved in 30 mL of THF. The disappearance of the infrared peak at 2189 cm^{-1} was monitored as the solution was refluxed for 24 h, and the color slowly changed from deep purple to orange-brown. After evaporation of the solvent, the product was extracted with diethyl ether and filtered. Addition of an equal volume of hexane to the rapidly stirring filtrate gave 130 mg of red-orange crystalline $PPN[Ru_4N(CO)_{12}]$ (79%).

B. $PPN[Ru(CO)_3(NO)]$ (38.8 mg, 0.0515 mmol) and $Ru_3(CO)_{12}$ (36.2 mg, 0.0566 mmol) were dissolved in 10 mL of THF and allowed to stir at room temperature for 12 h. The THF was removed under vacuum, and the residue was extracted with 2 × 10 mL of diethyl ether. The product was crystallized by adding an equal volume of hexane to the rapidly stirring filtrate. This gave 26 mg of orange crystals of $PPN[Ru_4N(CO)_{12}]$ (38%). Anal. Calcd: C, 44.59; H, 2.34; N, 2.17. Found: C, 44.03; H, 2.56; H, 2.06.

Kinetic Analysis of the Conversion of $PPN[Ru_4(NCO)(CO)_{13}]$ to $PPN[Ru_4N(CO)_{12}]$. For these experiments, a special Schlenk tube with a built-in condenser was used to minimize evaporation problems. In a typical experiment, the concentration of a THF solution of $PPN[Ru_4(NCO)(CO)_{13}]$ was determined by using a calibration curve of percent transmittance at 2189 cm^{-1} vs. concentration. The Schlenk tube was lowered into a thermostated water bath (±0.2 °C). Samples were withdrawn, and the reaction was monitored for a minimum of 2 half-lives. Experiments were run at three concentrations in refluxing THF (67 °C) and were in good agreement. Linear plots of $\ln[Ru_4(NCO)(CO)_{13}]$ vs. time indicated clean first-order kinetics for the reaction, with $k = (2.9 \pm 1.1) \times 10^{-5}$ s^{-1}.

Reactions of $PPN[Ru_4N(CO)_{12}]$ with CO. $PPN[Ru_4N(CO)_{12}]$ (20.0 mg, 0.0151 mmol) was dissolved in 20 mL of THF and pressurized to 3000 psig of CO. The solution was heated to 86 °C, and aliquots were removed at regular intervals. Infrared spectra of the removed samples indicated the formation of the isocyanate $PPN[Ru_3(NCO)(CO)_{11}]$ after 3 h, although unreacted $PPN[Ru_4N(CO)_{12}]$ still remained. Continued reaction led to a decrease in $PPN[(Ru_4N(CO)_{12}]$ concentration and formation of $[HRu_3(CO)_{11}]^-$, but no increase in the height of the $[Ru_3(NCO)(CO)_{11}]^-$ peaks at 2230 and 1830 cm^{-1}. After 6 h, the only clusters present were $[Ru_3(NCO)(CO)_{11}]^-$ and $[HRu_3(CO)_{11}]^-$.

Reaction of Metal Clusters with $Ru(CO)_5$. $Ru_3(CO)_{12}$ (49.6 mg, 0.0776 mmol) was suspended in 5 mL of THF and pressurized to 4100 psig of CO in a rocking autoclave. A temperature of 100 °C was maintained for 24 h. After the autoclave was cooled to room temperature, aliquots of the pale yellow THF solution of $Ru(CO)_5$ were syringed into a THF solution containing a stoichiometric amount of the appropriate clusters. The concentration of $Ru(CO)_5$ was approximately 0.07 M. An infrared spectrum was taken immediately after addition of $Ru(CO)_5$, and the reactions were monitored by infrared spectroscopy until completion. The results are listed individually below.

1. $[Ru_3(NCO)(CO)_{10}]^- + [Ru_3(NCO)(CO)_{11}]^- + Ru(CO)_5$. Immediately following addition of the $Ru(CO)_5$ to a mixture of the trimer isocyanates, the color of the solution changed from red to purple. The infrared spectrum indicated the formation of $[Ru_4(NCO)(CO)_{13}]^-$, with small amounts of unreacted $[Ru_3(NCO)(CO)_{11}]^-$ remaining.

2. $[Ru_4N(CO)_{12}]^- + Ru(CO)_5$. The addition of $Ru(CO)_5$ to a solution of $[Ru_4N(CO)_{12}]^-$ resulted in the slow formation of

(15) Levy, G. C.; Lichter, R. L. "Nitrogen-15 Nuclear Magnetic Resonance Spectroscopy"; Wiley: New York, 1979.
(16) Smieja, J. A.; Stevens, R. E.; Fjare, D. E.; Gladfelter, W. L., to be submitted for publication.

Table II. Summary of Crystallographic Data

Crystal Parameters

cryst system: triclinic	space group: $P\bar{1}$
a = 12.123 (6) Å	V = 1754 (2) Å^3
b = 14.263 (5) Å	Z = 2
c = 10.642 (3) Å	d(calcd) = 2.14 g cm^{-3}
α = 104.74 (3) Å	temp = 23 °C
β = 93.28 (3) Å	abs coeff = 21.2 cm^{-1}
γ = 80.25 (4) Å	

Measurement of Intensity Data

diffractometer: Enraf-Nonius CAD4
radiation: Mo Kα (λ = 0.710 73 Å)
monochromator: graphite crystal
scan type: ω-2θ
scan speed: variable from 0.6 to 20°/min
scan range: 0° ≤ 2θ ≤ 36°
reflcns measd: $+h,\pm k,\pm l$
reflcns collected: 2317 unique reflcns, 1437 with $I > 2\sigma(I)$
check reflcns: {00$\bar{6}$}, {0$\bar{7}$0}, {413} measd approximately every 80 reflcns
p = 0.06
R = 0.068
R_w = 0.074
error in observn of unit weight: 1.701

$[Ru_5N(CO)_{14}]^-$. The reaction was complete after 90 min at room temperature.

3. $[Ru_5N(CO)_{14}]^-$ + $Ru(CO)_5$. The only reaction occurring upon the addition of $Ru(CO)_5$ to a solution of $[Ru_5N(CO)_{14}]^-$ was the condensation of the $Ru(CO)_5$ to form $Ru_3(CO)_{12}$.

PPN[$Ru_5N(CO)_{14}$] + $^1/_3Ru_3(CO)_{12}$. PPN[$Ru_5N(CO)_{14}$] (9.6 mg, 0.0059 mmol) and $Ru_3(CO)_{12}$ (3.8 mg, 0.0059 mmols) were dissolved in 10 mL of THF. The solution was refluxed for 24 h, when the infrared spectrum indicated clean conversion to PPN-$[Ru_6N(CO)_{16}]$.

3PPN[$Ru_4(NCO)(CO)_{13}$] + 2$Ru_3(CO)_{12}$. PPN[$Ru_4(NCO)(CO)_{13}$] (14.5 mg, 0.0107 mmol) and $Ru_3(CO)_{12}$ (9.2 mg, 0.0144 mmol) were dissolved in 10 mL of THF. The solution was refluxed for 13 h, at which time the infrared spectrum indicated complete conversion to PPN$[Ru_6N(CO)_{16}]$.

PPN[$Ru_6N(CO)_{16}$] + High Pressures of CO. PPN[$Ru_6N(CO)_{16}$] (21.2 mg, 0.0132 mmol) was dissolved in 3 mL of THF, pressurized to 3000 psig, and heated to 70 °C in a rocking autoclave. After 3 h, the system was cooled and depressurized and the clusters $[Ru_5N(CO)_{14}]^-$, $[Ru_3(NCO)(CO)_{11}]^-$, and $[Ru_4(NCO)(CO)_{13}]^-$ were detected by infrared spectroscopy. Peaks that could be attributed to $[Ru_4N(CO)_{12}]^-$ were observed at 2032 and 1999 cm^{-1}; however, due to the complexity of the terminal carbonyl region, a definite assignment cannot be made. Further reaction occurred at room temperature as the $[Ru_3(NCO)(CO)_{11}]^-$ condensed with the $Ru(CO)_5$ generated from cluster fragmentation, leaving $[Ru_4(NCO)(CO)_{13}]^-$ as the only isocyanate-containing product.

Collection and Reduction of the X-ray Data for [$PhCH_2Et_3N$][$Ru_5N(CO)_{14}$]. Red crystals of the compound were grown from a solution of ether/hexane. A suitable, approximately equidimensional (0.2 mm) crystal was chosen and sealed in a glass capillary. The crystal was found to be triclinic by the Enraf-Nonius CAD4-SDP peak search, centering, and indexing programs and by a Delauney reduction calculation.[17] The centric space group $P\bar{1}$ was chosen, and data collection was begun. Table II summarizes the crystal data and intensity measurement parameters. Background counts were measured at both ends of the scan range with the use of an ω–2θ scan, equal at each side to one-fourth of the scan range of the peak. In this manner the total duration of measuring background is equal to one-half of the time required for the peak scan. The check reflections indicated a severe problem with decay of the crystal in the X-ray beam. Although we limited data collection to 36° in 2θ, the reflections dropped to 31% of their original intensity. The data were corrected for this decay as well as for Lorentz, polarization, and background effects but not for absorption.[18] Due to the decay problem the quality of the data and the subsequent structural details are limited.

Solution and Refinement of the Structure. The structure was solved by conventional heavy-atom techniques. The positions of the ruthenium atoms were located by a Patternson synthesis. Following several cycles of least-squares refinement, followed by difference Fourier calculations, the positions of all atoms were readily located. The refinement was continued to convergence by using anisotroic temperature factors for the metal atoms.[19] The values of the atomic scattering factors used in the calculations were taken from the usual tabulation, and the effects of anomalous dispersion were included.[20] Tables III–V contain the positional parameters, bond distances, and bond angles, respectively.

Results

Conversions of Isocyanates to Nitrides. The direct formation of $[Ru_4N(CO)_{12}]^-$ from $[Ru_4(NCO)(CO)_{13}]^-$ occurs smoothly in refluxing THF in 24 h. The new tetranuclear nitrido cluster was characterized by infrared and ^{15}N NMR spectroscopy, elemental analysis, and its conversion into a known cluster. It can also be prepared by an independent procedure discussed below. The infrared spectrum in THF exhibits four bands in the terminal carbonyl region (similar to $[Fe_4N(CO)_{12}]^-$)[21] and no bridging carbonyl peaks. The ^{15}N NMR resonance appears at 519.1 ppm which is 99 ppm upfield from that found in the analogous iron cluster. Protonation of $[Ru_4N(CO)_{12}]^-$ with CF_3SO_3H ultimately leads to $HRu_4N(CO)_{12}$, which has been previously characterized by X-ray crystallography as its $P(OCH_3)_3$ derivative.[22]

The conversion of $[Ru_4(NCO)(CO)_{13}]^-$ into $[Ru_4N(CO)_{12}]^-$ can be easily followed by using infrared spectroscopy. No intermediates are detectable in this conversion, and the ν_{NCO} band at 2189 cm^{-1} provided a convenient method to determine the kinetics of this reaction. In the concentration range from 0.45 to 1.0 mM in THF at 67 °C the disappearance of $[Ru_4(NCO)(CO)_{13}]^-$ followed first-order kinetics for 2 half-lives. The observed rate constant was $(2.9 \pm 1.1) \times 10^{-5}$ s^{-1}. Experiments to test the effect of added CO on the rate were not feasible because $[Ru_4(NCO)(CO)_{13}]^-$ rapidly forms $[Ru_3(NCO)(CO)_{11}]^-$ and $^1/_3Ru_3(CO)_{12}$ under a CO atmosphere at room temperature.[12]

When 1 equiv of $PPN(N_3)$ is added to 2 equiv of $Ru_3(CO)_{12}$ and the resulting mixture refluxed, the hexanuclear cluster $[Ru_6N(CO)_{16}]^-$ is formed in high yield. The initial reaction of azide with 1 equiv of $Ru_3(CO)_{12}$ is complete within minutes at room temperature, giving a mixture of

(17) All calculations were carried out on PDP 8A and 11/34 computers using the Enraf-Nonius CAD 4-SDP programs. This crystallographic computing package is described in: Frenz, B. A. In "Computing in Crystallography"; Schenk, H., Olthof-Hazekamp, R., van Koningsveld, H., Bassi, G. C., Eds.; Delft University Press: Delft, Holland, 19788; pp 64–71. See also: "CAD 4 and SDP User's Manual"; Enraf-Nonius: Delft, Holland, 1978.

(18) The intensity data were processed as described: "CAD 4 and SDP User's Manual"; Enraf-Nonius: Delft, Holland, 1978. The net intensity $I = (K/\text{NPI})(C - 2B)$, where K = 20.1166 × (attenuator factor), NPI = ratio of fastest possible scan rate to scan rate for the measurement, C = total count, and B = total background count. The standard deviation in the net intensity is given by $\sigma^2(I) = (K/\text{NPI})^2[C + 4B + (pI)^2]$, where p is a factor used to downweight intense reflections. The observed structure factor amplitude F_o is given by $F_3 = (I/Lp)^{1/2}$, where Lp = Lorentz and polarization factors. The $\sigma(I)$'s were converted to the estimated errors in the relative structure factors $\sigma(F_o)$ by $\sigma(F_o) = {}^1/_2(\sigma(I)/I)F_o$.

(19) The function minimized was $\sum w(|F_o| - |F_c|)^2$, where $w = 1/\sigma^2(F_o)$. The unweighted and weighted residuals are defined as $R = (\sum||F_o| - |F_c||)/\sum|F_o|$ and $R_w = [(\sum w(|F_o| - |F_c|))^2/(\sum w|F_o|)^2]^{1/2}$. The error in an observation of unit weight is $[\sum w(|F_o| - |F_c|)^2/(\text{NO} - \text{NV})]^{1/2}$, where NO and NV are the number of observations and variables, respectively.

(20) Cromer, D. T.; Waber, J. T. "International Tables for X-ray Crystallography"; Kynoch Press: Birmingham, England, 1974; Vol. IV, Table 2.2A. Cromer D. T. *Ibid.*, Table 2.3.1.

(21) Fjare, D. E.; Gladfelter, W. L. *Inorg. Chem.* **1981**, *20*, 3533–3539.

(22) Braga, D.; Johnson, B. F. G.; Lewis, J.; Mace, J. M.; McPartlin, M.; Puga, J.; Nelson, W. J. H.; Raithby, P. R.; Whitmire, K. H. *J. Chem. Soc., Chem. Commun.* **1982**, *1081*–1083.

Table III. Positional Parameters

atom	x	y	z	atom	x	y	z
Ru(1)	0.2946 (2)	0.3271 (2)	0.3501 (2)	C(21)	0.237 (2)	0.507 (2)	−0.022 (2)
Ru(2)	0.2559 (2)	0.3881 (2)	−0.0018 (2)	C(22)	0.269 (2)	0.352 (2)	−0.181 (2)
Ru(3)	0.1127 (2)	0.3479 (2)	0.1694 (2)	C(23B)	0.087 (2)	0.377 (2)	−0.003 (2)
Ru(4)	0.4396 (2)	0.3719 (2)	0.1838 (2)	C(31)	−0.002 (3)	0.280 (3)	0.155 (3)
Ru(5)	0.3188 (2)	0.2206 (2)	0.0962 (2)	C(32)	0.020 (3)	0.462 (3)	0.253 (3)
O(11)	0.269 (2)	0.516 (2)	0.567 (2)	C(41)	0.576 (4)	0.310 (3)	0.240 (4)
O(12)	0.472 (2)	0.218 (2)	0.496 (3)	C(42)	0.463 (3)	0.491 (2)	0.282 (3)
O(13)	0.112 (2)	0.237 (2)	0.437 (2)	C(43)	0.491 (3)	0.378 (2)	0.021 (3)
O(21)	0.217 (2)	0.592 (2)	−0.037 (2)	C(51)	0.430 (4)	0.138 (3)	0.171 (4)
O(22)	0.280 (2)	0.326 (2)	−0.289 (2)	C(52)	0.207 (3)	0.142 (2)	0.072 (3)
O(23B)	0.015 (2)	0.377 (2)	−0.092 (2)	C(53)	0.376 (2)	0.186 (2)	−0.073 (2)
O(31)	−0.077 (2)	0.236 (2)	0.151 (2)	C(61)	0.335 (3)	−0.142 (3)	0.341 (4)
O(32)	−0.034 (2)	0.527 (2)	0.322 (2)	C(62)	0.362 (4)	−0.036 (3)	0.372 (4)
O(41)	0.652 (2)	0.271 (2)	0.284 (2)	C(63)	0.197 (3)	−0.090 (3)	0.164 (3)
O(42)	0.475 (2)	0.572 (2)	0.342 (2)	C(64)	0.298 (3)	−0.149 (2)	0.056 (3)
O(43)	0.542 (2)	0.380 (1)	−0.065 (2)	C(65)	0.181 (4)	−0.239 (3)	0.227 (4)
O(51)	0.499 (2)	0.082 (2)	0.191 (2)	C(66)	0.190 (3)	−0.295 (3)	0.348 (3)
O(52)	0.146 (2)	0.087 (2)	0.041 (2)	C(67)	0.126 (2)	−0.070 (2)	0.377 (2)
O(53)	0.419 (2)	0.155 (1)	−0.172 (2)	C(68)	−0.001 (4)	−0.060 (3)	0.324 (4)
N(1)	0.277 (2)	0.374 (2)	0.186 (2)	C(69)	−0.075 (2)	−0.124 (2)	0.329 (2)
N(2)	0.208 (2)	−0.138 (2)	0.269 (2)	C(70)	−0.188 (3)	−0.098 (2)	0.316 (3)
C(11)	0.277 (3)	0.441 (2)	0.478 (3)	C(71)	−0.221 (3)	−0.006 (3)	0.289 (3)
C(12)	0.408 (3)	0.259 (2)	0.445 (3)	C(72)	−0.154 (3)	0.054 (2)	0.271 (3)
C(13)	0.175 (3)	0.275 (3)	0.392 (3)	C(73)	−0.037 (3)	0.034 (3)	0.292 (3)

Table IV. Bond Distances (Å)

Ru(1)-Ru(3)	2.868 (4)	Ru(3)-C(32)	1.86 (3)
Ru(1)-Ru(4)	2.818 (3)	Ru(4)-C(41)	1.88 (4)
Ru(1)-Ru(5)	2.747 (3)	Ru(4)-C(42)	1.81 (3)
Ru(2)-Ru(3)	2.809 (3)	Ru(4)-C(43)	1.90 (2)
Ru(2)-Ru(4)	2.911 (4)	Ru(5)-C(51)	1.91 (4)
Ru(2)-Ru(5)	2.817 (3)	Ru(5)-C(52)	1.87 (3)
Ru(3)-Ru(5)	2.848 (3)	Ru(5)-C(53)	1.89 (2)
Ru(4)-Ru(5)	2.751 (4)	C(11)-O(11)	1.24 (3)
Ru(1)-N(1)	2.01 (2)	C(12)-O(12)	1.10 (3)
Ru(2)-N(1)	2.06 (2)	C(13)-O(13)	1.19 (3)
Ru(3)-N(1)	2.07 (2)	C(21)-O(21)	1.25 (3)
Ru(4)-N(1)	1.97 (2)	C(22)-O(22)	1.12 (2)
Ru(5)-N(1)	2.14 (2)	C(23B)-O(23B)	1.26 (3)
Ru(1)-C(11)	1.82 (3)	C(31)-O(31)	1.19 (3)
Ru(1)-C(12)	1.94 (3)	C(32)-O(32)	1.15 (3)
Ru(1)-C(13)	1.86 (3)	C(41)-O(41)	1.14 (4)
Ru(2)-C(21)	1.74 (3)	C(42)-O(42)	1.20 (3)
Ru(2)-C(22)	1.85 (2)	C(43)-O(43)	1.14 (3)
Ru(2)-C(23B)	2.07 (2)	C(51)-O(51)	1.11 (4)
Ru(3)-C(31)	1.80 (4)	C(52)-O(52)	1.15 (3)
Ru(3)-C(23B)	1.98 (2)	C(53)-O(53)	1.15 (2)

the trimer isocyanate clusters $[Ru_3(NCO)(CO)_{11}]^-$ and $[Ru_3(NCO)(CO)_{10}]^-$.[12] The conversion of these into $[Ru_6N(CO)_{16}]^-$ appears to take place by two paths. In the reaction, $[Ru_6N(CO)_{16}]^-$ is formed rapidly (1 h). At the same time, some of the trimers are converted into $[Ru_4(NCO)(CO)_{13}]^-$. In the presence of excess $Ru_3(CO)_{12}$, this tetramer is also converted to $[Ru_6N(CO)_{16}]^-$ but on a much slower time scale. We were not able to detect any additional intermediates in this reaction using infrared spectroscopy.

The new cluster was characterized by using infrared, ^{13}C NMR, and ^{15}N NMR spectroscopy, elemental analysis, and mass spectrometry. Using the fast atom bombardment mass spectral technique (FAB/MS), a negative ion peak at m/s 1074 (^{102}Ru) and a positive ion peak at m/s 538 were observed consistent with the formulation of the salt as $PPN[Ru_6N(CO)_{16}]$. The infrared spectrum was very simple which is often the case with larger clusters having relatively high symmetry. One intense peak is found in the terminal CO region at 2010 cm^{-1} and one weak peak in the bridging CO region at 1839 cm^{-1}. The ^{13}C NMR gives one resonance at 206.7 ppm down to −80 °C indicative of a facile CO exchange process. $[Ru_6N(CO)_{16}]^-$ could also be quantitatively converted into a structurally characterized cluster as discussed below.

Nitrosyl to Nitride Conversions. Both $[Ru_4N(CO)_{12}]^-$ and $[Ru_6N(CO)_{16}]^-$ can be prepared using precedented routes for nitrido cluster formation. The reaction of NO^+ with $[Ru_6(CO)_{18}]^{2-}$ leads to $[Ru_6N(CO)_{16}]^-$ in 38% yield. The reaction is conducted in CH_2Cl_2 initially at low temperature and then is allowed to warm to room temperature. After 12 h the solvent was removed and the product was crystallized from ether/hexane. Following this reaction using infrared spectroscopy does not allow the observation of any intermediate nitrosyl complexes.

The redox condensation between a mononuclear nitrosyl complex and a trimetallic cluster has also been used to generate nitrido clusters.[21] When the recently reported[14] nitrosyl carbonylmetalate $[Ru(CO)_3(NO)]^-$ is reacted with $Ru_3(CO)_{12}$ at room temperature for 12 h, $[Ru_4N(CO)_{12}]^-$ is formed and can be isolated in 38% yield. As in the above reaction no intermediates have been detected in this synthesis.

Nuclearity Changes among the Clusters. The addition and/or removal of a "$Ru(CO)_2$" moiety is a char-

Table V. Selected Angles (deg)

Ru(1)-Ru(3)-Ru(2)	90.7 (1)	Ru(4)-Ru(1)-Ru(5)	59.24 (8)	Ru(3)-Ru(1)-N(1)	46.2 (6)
Ru(1)-Ru(3)-Ru(5)	57.45 (8)	Ru(1)-N(1)-Ru(3)	89.4 (7)	Ru(3)-Ru(5)-N(1)	46.4 (6)
Ru(1)-Ru(4)-Ru(2)	89.7 (1)	Ru(1)-N(1)-Ru(4)	90.1 (8)	Ru(4)-Ru(1)-N(1)	44.5 (6)
Ru(1)-Ru(5)-Ru(2)	93.09 (9)	Ru(1)-N(1)-Ru(5)	83.0 (7)	Ru(5)-Ru(1)-N(1)	50.5 (5)
Ru(1)-Ru(5)-Ru(3)	61.65 (8)	Ru(3)-N(1)-Ru(5)	85.3 (8)	Ru(5)-Ru(3)-N(1)	48.3 (5)
Ru(1)-Ru(5)-Ru(4)	61.66 (8)	Ru(1)-Ru(3)-N(1)	44.5 (5)	Ru(2)-C(23B)-O(23B)	130 (1)
Ru(2)-Ru(3)-Ru(5)	59.73 (8)	Ru(1)-Ru(5)-N(1)	46.6 (5)	Ru(3)-C(23B)-O(23B)	141 (2)
Ru(3)-Ru(1)-Ru(4)	90.15 (9)	Ru(2)-Ru(3)-N(1)	46.9 (5)	Ru(2)-C(23B)-Ru(3)	88 (1)
Ru(3)-Ru(5)-Ru(4)	92.0 (1)				

acteristic reaction of the clusters discussed in this paper. The most facile reaction of this type is the conversion of $[Ru_6N(CO)_{16}]^-$ to $[Ru_5N(CO)_{14}]^-$ (eq 4), which occurs quantitatively within a few minutes at room temperature. The ruthenium carbonyl group cleaved from the cluster trimerizes to form $Ru_3(CO)_{12}$.

$$[Ru_6N(CO)_{16}]^- + 2CO \xrightarrow{25\ °C} [Ru_5N(CO)_{14}]^- + {}^1/_3Ru_3(CO)_{12} \quad (4)$$

The new pentanuclear nitrido cluster formed in this reaction was characterized using spectroscopic techniques and a single-crystal X-ray crystallographic analysis of the benzyltriethylammonium salt discussed below. No further reaction of $[Ru_5N(CO)_{14}]^-$ with CO occurs until high pressures are used. When $[Ru_6N(CO)_{16}]^-$ is dissolved in THF and heated to 70 °C at 3000 psig of CO for 3 h, a mixture of compounds results. $[Ru_5N(CO)_{14}]^-$ is the predominant species, while $[Ru_4N(CO)_{12}]^-$ and $[Ru_4(NCO)(CO)_{13}]^-$ are also present in approximately equal amounts. Separation of these monoanions was not possible by crystallization, and the overlapping infrared bands makes the verification of the presence of $[Ru_4N(CO)_{12}]^-$ difficult. However, the appearance of an absorbance at 2032 cm^{-1} cannot be attributed to either $[Ru_5N(CO)_{14}]^-$ or $[Ru_4(NCO)(CO)_{13}]^-$, while this does correspond to one of the intense absorptions in $[Ru_4N(CO)_{12}]^-$. It is reasonable to suggest that the $[Ru_4N(CO)_{12}]^-$ originates from the reaction of $[Ru_5N(CO)_{14}]^-$ with CO.

Starting with $[Ru_4N(CO)_{12}]^-$ both $[Ru_5N(CO)_{14}]^-$ and $[Ru_6N(CO)_{16}]^-$ can be synthesized by the addition of ruthenium carbonyl fragments. When $Ru(CO)_5$ in THF is added to $[Ru_4N(CO)_{12}]^-$, the pentanuclear cluster is formed at room temperature (eq 5). The further addition of $Ru(CO)_5$ does not result in the formation of the hexanuclear cluster, and if the temperature is even slightly raised the $Ru(CO)_5$ rapidly forms $Ru_3(CO)_{12}$.

$$[Ru_4N(CO)_{12}]^- + Ru(CO)_5 \rightarrow [Ru_5N(CO)_{14}]^- + 3CO \quad (5)$$

Triruthenium dodecacarbonyl itself can be used as the source of the "$Ru(CO)_2$" fragment. However, the reactions required refluxing THF and times up to 24 h to complete the conversion to $[Ru_6N(CO)_{16}]^-$ (eq 6 and 7).

$$3[Ru_4N(CO)_{12}]^- + 2Ru_3(CO)_{12} \rightarrow 3[Ru_6N(CO)_{16}]^- + 12CO \quad (6)$$

$$[Ru_5N(CO)_{14}]^- + {}^1/_3Ru_3(CO)_{12} \rightarrow [Ru_6N(CO)_{16}]^- + 2CO \quad (7)$$

Changes in nuclearity among the isocyanato-containing clusters have been previously reported.[12] One new reaction that is pertinent to the current study is the trimer to tetramer conversion (eq 8) using $Ru(CO)_5$. This reaction occurs upon mixing the two reagents at room temperature.

$$[Ru_3(NCO)(CO)_{10}]^- + Ru(CO)_5 \rightarrow [Ru_4(NCO)(CO)_{13}]^- + 2CO \quad (8)$$

Nitride to Isocyanate Conversions. When a THF solution of $[Ru_4N(CO)_{12}]^-$ is pressurized with CO to 3000 psig at 86 °C, the infrared spectrum indicates the slow formation of $[Ru_3(NCO)(CO)_{11}]^-$. The unique absorptions due to this cluster grow in at 2230 and 1830 cm^{-1}. After 6 h all of the $[Ru_4N(CO)_{12}]^-$ was consumed, and the infrared spectrum indicated indicated the presence of $[Ru_3(NCO)(CO)_{11}]^-$ and a second species ultimately identified as $[HRu_3(CO)_{11}]^-$. This assignment is based on the characteristic infrared absorptions at 2012 s, 1984 s, 1947 m, and particularly 1725 w cm^{-1}. The source of the hydrogen is presumably from small amounts of hydrogen present in the CO that react with $[Ru_3(NCO)(CO)_{11}]^-$.[23] Within a few minutes after the CO pressure is released, $[Ru_3(NCO)(CO)_{11}]^-$ partially converts to $[Ru_4(NCO)(CO)_{13}]^-$ presumably via reaction with $Ru(CO)_5$. Likewise the $[HRu_3(CO)_{11}]^-$ is rapidly converted to $[HRu_4(CO)_{13}]^-$. The conversion of the nitride into the isocyanato ligand in these ruthenium clusters does require both increased temperature (≥70 °C) and pressure conditions. No reaction was observed when the temperature was lowered to 25 °C while the CO pressure was maintained at 3000 psig. Other conditions (67 °C, 15 psig of CO; 70 °C, 50 psig of CO) also resulted in no reaction.

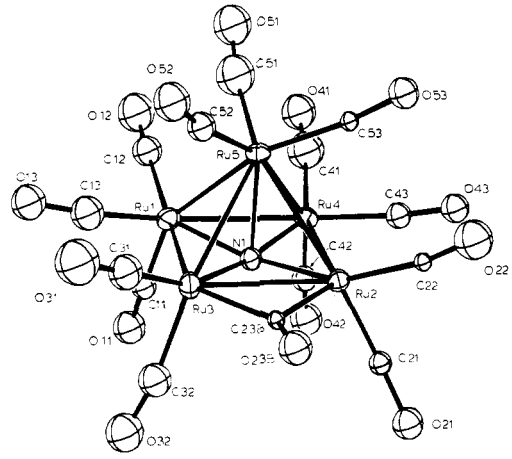

Figure 1. View of $[Ru_5N(CO)_{14}]^-$ with the atomic labeling scheme.

The reaction of $[Ru_6N(CO)_{16}]^-$ with CO (70 °C, 3000 psig of CO, 3 h) also results in isocyanate formation as mentioned above. Since two ruthenium carbonyl groups are converted into $Ru(CO)_5$ as the nuclearity of starting cluster is lowered, the isolation of $[Ru_4(NCO)(CO)_{13}]^-$ is not surprising.

Structure of $[Ru_5N(CO)_{14}]^-$. A view of the anion is shown in Figure 1, and lists of the distances and selected bond angles are given in Tables IV and V. The structure consists of well-separated anions and cations. The anion contains five ruthenium atoms in a square-pyramidal arrangement with the nitrogen atom situated 0.21 (2) Å below the basal plane of ruthenium atoms. The Ru–N distances are separated into three sets. The longest is the distance from the N to the apical Ru atom (Ru(5)–N) at 2.14 (2) Å. The Ru(2/3)–N distances are 2.06 (2)/2.07 (2) Å, and the Ru(1/4)–N distances are 2.01 (2) and 1.97 (2) Å, respectively. The Ru–Ru bond distances vary from 2.747 (3) to 2.911 (4) Å. Because of the decay problem of this crystal, the errors associated with the carbonyl ligands and the cation, in particular, are larger than normal. Despite that, we were able to easily locate and refine all of the atoms of the structure. The average Ru–C distance for the terminal ligands is 1.86 (5) Å, and the average C–O distance is 1.16 (5) Å. The Ru–C–O angles of the terminal ligands average 173 (4)°. There is one bridging carbonyl that lies on the pseudo mirror-plane of symmetry of the anion.

Discussion

Structure and Spectroscopic Properties of the Nitrido Clusters. The three clusters in this homologous series, $[Ru_6N(CO)_{16}]^-$, $[Ru_5N(CO)_{14}]^-$, and $[Ru_4N(CO)_{12}]^-$, are proposed to be related by the sequential removal of a $Ru(CO)_2$ group from an apex of an octahedron (Scheme

(23) Gladfelter, W. L. In "Organometallic Compounds: Synthesis, Structure, and Reactivity"; Shapiro, B. L., Ed.; Texas A&M University Press: College Station, TX 1983; p 281.

Scheme I

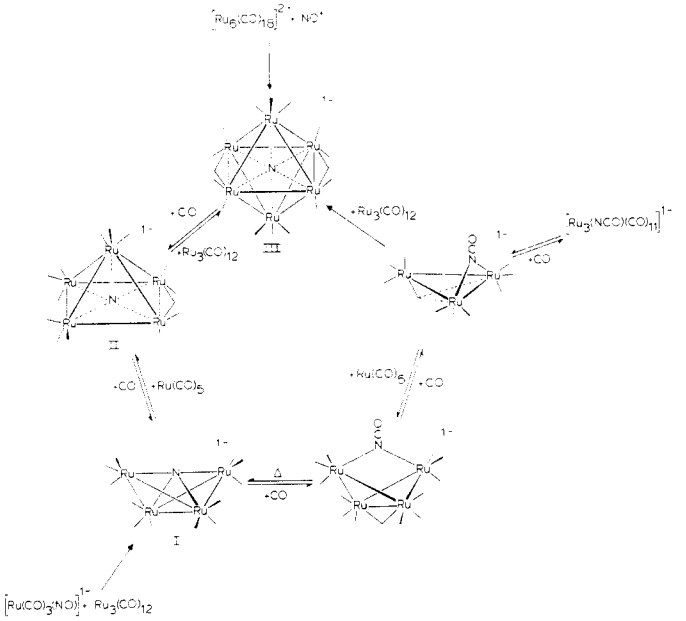

I). The structure of the pentaruthenium nitrido cluster is similar to several other M_5X clusters where the central element (C or N) is located in the square face of a square-based pyramid. The only other structurally characterized M_5N species are $HFe_5N(CO)_{14}$[24] (IV) and $[Fe_5N(CO)_{14}]^-$,[25] where the former differs from $[Ru_5N(CO)_{14}]^-$

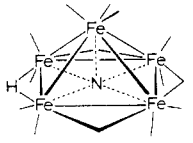

IV

in that it contains four bridging ligands around the basal plane. The distribution of CO ligands in $[Ru_5N(CO)_{14}]^-$ is the same as found in $[Fe_4RhC(CO)_{14}]^{2-}$[26] and $[Fe_5N(CO)_{14}]^-$. In each of these M_5N clusters the nitrogen to basal metal atom distances are shorter than the nitrogen to apical metal atom distance, and the position of the nitrogen lies below the plane of basal metal atom. This value is 0.21 Å for $[Ru_5N(CO)_{14}]^-$, and the corresponding value in $HFe_5N(CO)_{14}$ is 0.093 Å.[24]

There are some interesting differences beginning to appear in the comparison between N and C in these clusters. In particular, we note that it is much easier to go from $[Ru_6N(CO)_{16}]^-$ to $[Ru_5N(CO)_{14}]^-$ under CO than it is to convert $Ru_6C(CO)_{17}$ into $Ru_5C(CO)_{15}$. The latter reaction requires 1200 psig of CO at 70 °C for 3 h. Further reduction in nuclearity from $[Ru_5N(CO)_{14}]^-$ to $[Ru_4N(CO)_{12}]^-$ is observed, while the analogous cluster $Ru_4C(CO)_{13}$ cannot be isolated from $Ru_5C(CO)_{15}$.[27] Since $[Ru_6C(CO)_{16}]^{2-}$ is similarly unreactive under a CO atmosphere,[28] it is likely that these reactivity differences arise from the difference between the central element, rather than differences in the charge or number of CO ligands on the cluster. Another difference is that there are no reported three-coordinate carbido clusters, while the family of compounds with the formula $(\eta^5\text{-}C_5H_5)_3M_3(N)(O)(CO)_4$ (M = Mo and W) does contain a three-coordinate nitrogen.[29] In cases where the synthesis of a M_3C cluster has been attempted the stable product contains the ketenylidene (CCO) ligand.[30] Lastly, in the high nuclearity cluster $[Rh_{10}PtN(CO)_{21}]^{3-}$, nitrogen is found to be five-coordinate.[31] It was pointed out that in large carbido clusters, carbon usually occupies sites with coordination numbers of six to eight. In $[Rh_{10}PtN(CO)_{21}]^{3-}$, the nitrogen has forced the reduction of the overall compactness of the cluster to achieve five-coordination.

All of the above observations point to the preference of nitrogen for lower coordination numbers relative to carbon. The smaller size of the nitrogen atom makes it increasingly difficult to fit larger numbers of metals around it, while a good bonding distance is maintained to each of the metals. Besides the smaller size, it also seems reasonable that the ability of the more electronegative element to stabilize the lone pair of electrons contributes to the trend. An extension of this trend to the next element over, oxygen, also seems to follow this pattern. Several examples of carbonyl clusters with mono-, di-, or tricoordinate oxygen atoms are known,[32-36] while no examples of higher coordination numbers currently exist for low-valent clusters.

The structure of the remaining two nitrido clusters reported in this study are based on spectroscopic evidence and their relationship to structurally characterized species. The butterfly structure is currently the most common geometry observed in nitrido clusters. The spectroscopic evidence and the chemical reactivity of $[Ru_4N(CO)_{12}]^-$ leave no doubt that its structure, I, is the same as $[Fe_4N(CO)_{12}]^-$[20] and $[Os_4N(CO)_{12}]^-$,[37] both of which have been structurally characterized.

While there are no related nitrido clusters with octahedral metal atom geometry, several isoelectronic carbido clusters provide sufficient precedent for the proposed octahedral structure of $[Ru_6N(CO)_{16}]^-$. Specifically, $Ru_6C(CO)_{17}$ (V)[38] and $[Ru_6C(CO)_{16}]^{2-}$ (VI)[39] have 86 elec-

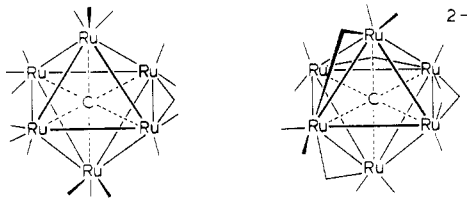

V VI

(24) Tachikawa, M.; Stein, J.; Muetterties, E. L.; Teller, R. G.; Beno, M. A.; Gebert, E.; Williams, J. M. *J. Am. Chem. Soc.* **1980**, *102*, 6648–6649.
(25) Gourdon, A.; Jeannin, R. *C.R. Hebd Seance Acad. Sci.* **1982**, *295*, 1101–1104.
(26) Tachikawa, M.; Sievert, A. C.; Muetterties, E. L.; Thompson, M. R.; Day, C. S.; Day, V. W. *J. Am. Chem. Soc.* **1980**, *102*, 1725–1727.
(27) Farrar, D. H.; Jackson, P. F.; Johnson, B. F. G.; Lewis, J.; Nicholls, J. N.; McPartlin, M. *J. Chem. Soc., Chem. Commun.* **1981**, 415–416.
(28) While a study focussing on the reaction of $[Ru_6C(CO)_{16}]^{2-}$ with CO has not been reported, the conversion of the dianion to $Ru_6C(CO)_{17}$ involves the addition of an oxidant to a solution of $[Ru_6C(CO)_{16}]^{2-}$ saturated with CO. No pentanuclear species were reported: Hayward, C. M. T.; Shapley, J. R. *Inorg. Chem.* **1982**, *21*, 3816.
(29) Feasey, N. D.; Knox, S. A. R.; Orpen, A. G. *J. Chem. Soc., Chem. Commun.* **1982**, 75–76.
(30) Kolis, J. W.; Holt, E. M.; Shriver, D. *J. Am. Chem. Soc.* **1983**, *105*, 7307–7313.
(31) Martinengo, S.; Ciani, G.; Sironi, A. *J. Am. Chem. Soc.* **1982**, *104*, 328–330.
(32) Goudsmit, M. A.; Johnson, B. F. G.; Lewis, J.; Raithby, P. R.; Whitmire, K. H. *J. Chem. Soc., Chem. Commun.* **1983**, 246–247.
(33) Ceriotti, A.; Resconi, L. *J. Organomet. Chem.* **1983**, *249*, C35–C37.
(34) Uchtman, V. A.; Dahl, L. F. *J. Am. Chem. Soc.* **1969**, *91*, 3763–3769.
(35) Bertolucci, A.; Freni, M.; Romiti, P.; Ciani, G.; Sironi, A.; Albano, V. G. *J. Organomet. Chem.* **1976**, *113*, C61–C64.
(36) Shapley, J. R.; Park, J. T.; Churchill, M. R.; Ziller, J. W.; Beanan, L. R. *J. Am. Chem. Soc.* **1984**, *106*, 1144–1145.
(37) Collins, M. A.; Johnson, B. F. G.; Lewis, J.; Mace, J. M.; Morris, J.; McPartlin, M.; Nelson, W. J. H.; Puga, J.; Raithby, P. R. *J. Chem. Soc., Chem. Commun.* **1983**, 689–691.

trons, as does $[Ru_6N(CO)_{16}]^-$, whereas $[Co_6N(CO)_{15}]^-$ has 90 electrons and adopts a trigonal-prismatic metal atom arrangement, VII.[40] The distribution of carbonyl ligands

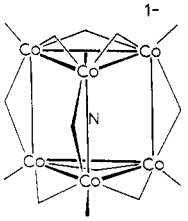

VII

in $[Ru_6N(CO)_{16}]^-$ is based on the structure of $Ru_6C(CO)_{17}$ and $[Ru_5N(CO)_{14}]^-$, as well as the need to evenly distribute the electrons around the structure. It fulfills the requirements set by the infrared spectrum for a structure with relatively high symmetry containing bridging carbonyls. We had hoped that the ^{13}C NMR spectrum would allow us to determine more about the structure, but even at −80 °C only one resonance is observed. A structure such as III does allow for a reasonable explanation for a low activation barrier CO exchange pathway. A pairwise bridging CO opening to a structure with all terminal ligands could be followed by pairwise bridge closure involving two different metals (eq 9). After a few such cycles all of the carbonyls would become equivalent. The ^{15}N NMR

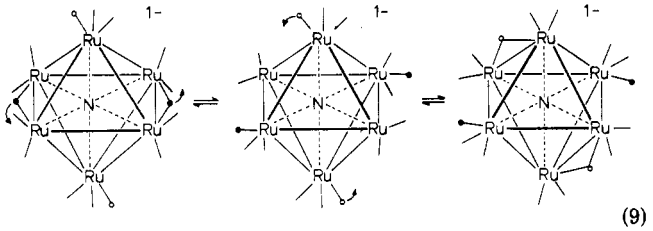

(9)

spectra (Table I) of these ruthenium clusters fall in the same region as other nitrido clusters of the iron triad but followed no simple pattern among each other. Of particular interest is the comparison between the chemical shift of $[Ru_6N(CO)_{16}]^-$ and the two other known hexanuclear nitrido clusters $[Co_6N(CO)_{15}]^-$ and $[Rh_6N(CO)_{15}]^-$. The chemical shifts of these clusters are 196.2 and 107.6 ppm, respectively,[40] which is upfield from the anticipated position based on the related carbido clusters. As a first approximation (ignoring the contribution from the ΔE term) the chemical shifts for nitrogen (measured relative to NH_4^+) are twice the value for carbon (measured relative to CH_4) for isoelectronic molecules.[41] This relationship arises from the comparison of the radial factors ($\langle r^{-3}\rangle_{2p}$) for nitrogen and carbon as it appears in the paramagnetic shielding term. Since the ^{13}C resonance for $[Co_6C(CO)_{15}]^{2-}$ appears at 332.8 ppm (relative to CH_4),[42] the unusual nature of the upfield shift in $[Co_6N(CO)_{15}]^-$ is particularly apparent. The $\delta_{^{15}N}$ for $[Ru_6N(CO)_{16}]^-$ appears at 538 ppm relative to NH_4^+, which can be compared to the carbon resonance of $[Ru_6C(CO)_{16}]^{2-}$ (461.2 ppm (CH_4)).[43] Although the $\delta_{^{15}N}$ value is not twice the $\delta_{^{13}C}$, it is at least larger than the carbon resonance. This fact further accentuates

Scheme II

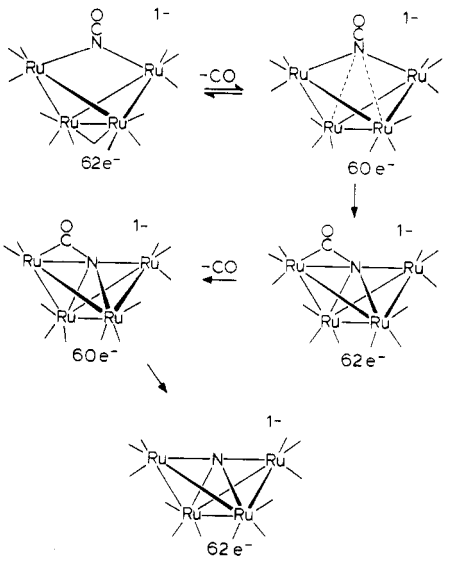

the unusual nature of the ^{15}N shifts in $[Co_6N(CO)_{15}]^-$ and $[Rh_6N(CO)_{15}]^-$. Several possible explanations have been discussed[44,45] to account for this, and it is clear that additional data is needed.

N–C Bond Formation and Cleavage. The transformation of greatest interest in this study is the isocyanate to nitride conversion and the reverse of this at high CO pressure. The conversion of $[Ru_4(NCO)(CO)_{13}]^-$ to $[Ru_4N(CO)_{12}]^-$ is conceptually the simplest reaction of this type, since there is no change in the nuclearity of the cluster. The kinetic study provides evidence that the reaction is first order in cluster concentration, which is consistent with a mechanism involving initial CO dissociation. However, we cannot conclusively rule out the possibility that initial fragmentation of $[Ru_4(NCO)(CO)_{13}]^-$ occurs followed by nitride formation and subsequent reformation of $[Ru_4N(CO)_{12}]^-$. Since $[Ru_4(NCO)(CO)_{13}]^-$ reacts instantly with CO,[12] inhibition studies to confirm a CO dissociation mechanism are not feasible. We believe that the fragmentation mechanism is unlikely, since the condensation to form the tetramer itself starts with the trimers. Further, previous studies of $[Ru_4(NCO)(CO)_{13}]^-$ found that it reacts quantitatively with H_2 to lose CO and form $[H_2Ru_4(NCO)(CO)_{12}]^-$.[12] Scheme II shows a sequence of events that could readily lead from $[Ru_4(NCO)(CO)_{13}]^-$ to $[Ru_4N(CO)_{12}]^-$. The actual mechanistic step whereby the carbon–nitrogen bond is ruptured is not rapidly reversed under these conditions. The experiment used to test this involved the pyrolysis of $[Ru_4(N^{13}CO)(CO)_{13}]^-$. The $N^{13}CO$ was approximately 62% ^{13}C enriched, and during the course of the conversion into $[Ru_4N(CO)_{12}]^-$ this ratio was not perceptibly altered. The infrared spectrum of the $[Ru_4N(CO)_{12}]^-$ did not exhibit any new absorptions that could be clearly labeled as a M–^{13}CO; however, the small amount of ^{13}CO involved would have made it difficult to detect once it scrambled with the remaining carbonyl ligands. This point will ultimately be important to address, since one mechanistic scheme for NCO dissociation is loss of CO directly to the gas phase. It is noteworthy that no scrambling of the ^{13}CO of the $N^{13}CO^-$ ligand occurred in the two trinuclear isocyanates or in their conversion into $[Ru_4(N^{13}CO)(CO)_{13}]^-$. This confirms the idea that no nitride

(38) Sirigu, A.; Bianchi, M.; Bendetti, E. *J. Chem. Soc., Chem. Commun.* **1969**, 596.
(39) Johnson, B. F. G.; Lewis, J.; Sankey, S. W.; Wong, K.; McPartlin, M.; Nelson, W. J. H. *J. Organomet. Chem.* **1980**, *191*, C3–C7.
(40) Martinengo, S.; Ciani, G.; Sironi, A.; Heaton, B. T.; Mason, J. *J. Am. Chem. Soc.* **1979**, *101*, 7095–7097.
(41) Mason, J. *Chem. Rev.* **1981**, *81*, 205–227.
(42) Albano, V. G.; Chini, P.; Ciani, G.; Sansoni, M.; Strumolo, D.; Heaton, B. T.; Martinengo, S. *J. Am. Chem. Soc.* **1976**, *98*, 5027.
(43) Bradley, J. S. *Adv. Organomet. Chem.* **1983**, *22*, 1–58.
(44) Heaton, B. T.; Strona, L.; Martinengo, S. *J. Organomet. Chem.* **1981**, *215*, 415–422.
(45) Mason, J. In Discussion in: Heaton, B. T. *Philos. Trans. R. Soc. Lond. A.* **1982**, *308*, 95–102.

intermediate is involved in the trimer to tetramer reaction.

The synthesis of $[Ru_6N(CO)_{16}]^-$ from the trimer isocyanates and $Ru_3(CO)_{12}$ clearly occurs in two steps. After the mixture is refluxed for 1 h, the only isocyanate cluster remaining is $[Ru_4(NCO)(CO)_{13}]^-$ and the only other clusters present in solution are $[Ru_6N(CO)_{16}]^-$ and some $Ru_3(CO)_{12}$. Approximately 22% of $[Ru_3(NCO)(CO)_{11}]^-$ is converted into $[Ru_4(NCO)(CO)_{13}]^-$ at this stage. The conversion of this remaining isocyanate into $[Ru_6N(CO)_{16}]^-$ occurs gradually over a period of 12 h, similar to the rate of conversion of $[Ru_4(NCO)(CO)_{13}]^-$ to $[Ru_4N(CO)_{12}]^-$. As suggested in Scheme I, we believe there is both a direct path (faster) from $[Ru_3(NCO)(CO)_{10}]^-$ and $Ru_3(CO)_{12}$ to $[Ru_6N(CO)_{16}]^-$ as well as an indirect route (slower) that proceeds through $[Ru_4(NCO)(CO)_{13}]^-$. It is possible that the direct condensation of $[Ru_3(NCO)(CO)_{10}]^-$ with $Ru_3(CO)_{12}$ is promoted by the isocyanate group that is capable of acting as a bridging ligand, and thereby stitching together the two trimers.

The reversion of the nitrido ligand back to the isocyanato ligand requires both elevated temperatures and high pressures of CO. Regardless of which nitrido cluster was initially charged in the reaction, it appears that $[Ru_4N(CO)_{12}]^-$ is the last detectable nitrido cluster present prior to isocyanate formation. While it is reasonable to suggest that the isocyanates are formed via a reverse of the mechanism shown in Scheme II, further fragmentation of $[Ru_4N(CO)_{12}]^-$ under high CO pressure cannot be ruled out.

The migration of CO to and from the nitrogen atom is related to several reactions discovered with carbido clusters,[46-53] and it seems probable that these are mechanistically similar. This reaction offers one of the most interesting and promising means of activating the usually reluctant nitride or carbide ligand in metal clusters. Further, in the case of nitrogen we have a reaction that is directly analogous to the surface reaction of nitrogen atoms with carbon monoxide.[7,8] By further study of these and related clusters we hope to be able to elucidate more on the mechanism of the CO migration.

Acknowledgment. We gratefully acknowledge the National Science Foundation for support of this work.

Registry No. I·PPN, 92845-78-8; II·PPN, 83312-28-1; II·$(PhCH_2Et_3N)$, 84809-77-8; III·PPN, 84809-76-7; PPN$[Ru_4(NCO)(CO)_{13}]$, 92845-79-9; PPN$[Ru_4(N^{13}CO)(CO)_{13}]$, 92845-75-5; PPN$[Ru_3(NCO)(CO)_{11}]$, 92900-63-5; $[Ru_3(N^{13}CO)(CO)_{11}]^-$, 92845-76-6; $[Ru_3(NCO)(CO)_{10}]^-$, 92900-64-6; $[Ru_3(N^{13}CO)(CO)_{10}]^-$, 92900-61-3; PPN$[Ru(CO)_3(NO)]$, 92845-81-3; $(PPN)_2[Ru_6(CO)_{18}]$, 62501-17-1; $[HRu_3(CO)_{11}]^-$, 60496-59-5; $Ru_3(CO)_{12}$, 15243-33-1; $Ru(CO)_5$, 16406-48-7; $NOPF_6$, 16921-91-8; NCO^-, 661-20-1.

Supplementary Material Available: Lists of calculated and observed structure factors, isotropic and anisotropic thermal parameters, and complete bond angles (16 pages). Ordering information is given on any current masthead page.

(46) Kolis, J. W.; Holt, E. M.; Drezdzon, M.; Whitmire, K. H.; Shriver, D. F. *J. Am. Chem. Soc.* **1982**, *104*, 6134–6135.
(47) Seyferth, D.; Hallgren, J. E.; Eschbach, C. S. *J. Am. Chem. Soc.* **1974**, *96*, 1730–1737.
(48) Bradley, J. S.; Ansell, G. B.; Hill, E. W. *J. Am. Chem. Soc.* **1979**, *101*, 7417–7419.
(49) Bradley, J. S.; Ansell, G. B.; Leonowicz, M. E.; Hill, E. W. *J. Am. Chem. Soc.* **1981**, *103*, 4968–4970.
(50) Keister, J. B.; Horling, T. L. *Inorg. Chem.* **1980**, *19*, 2304–2307.
(51) Davis, J. H.; Beno, M. A.; Williams, J. M.; Zimmie, J.; Tachikawa, M.; Muetterties, E. L. *Proc. Natl. Acad. Sci. U.S.A.* **1981**, *78*, 668–671.
(52) Sievert, A. C.; Strickland, D. S.; Shapley, J. R.; Steinmetz, G. R.; Geoffroy, G. L. *Organometallics* **1982**, *1*, 214–215.
(53) Arce, A. J.; Deeming, A. J. *J. Chem. Soc., Chem. Commun.* **1982**, *364*–365.

Dipotassium Bis([8]annulene)ytterbate(II) and -calcate(II)†

Steven A. Kinsley, Andrew Streitwieser, Jr.,* and Allan Zalkin*

Department of Chemistry, University of California, and Materials and Molecular Research Division, Lawrence Berkeley Laboratory, Berkeley, California 94720

Received June 5, 1984

The title compounds were prepared by stoichiometric reaction of cyclooctatetraene, potassium, and either ytterbium or calcium, in liquid ammonia solution. The dimethoxyethane adducts of $K_2[Yb(C_8H_8)_2]$ and $K_2[Ca(C_8H_8)_2]$ are crystalline and have similar X-ray powder patterns; $K_2[Yb(C_8H_8)_2]$ and $K_2[Ca(C_8H_8)_2]$ have identical infrared spectra. X-ray structure analysis of $[K(C_4H_{10}O_2)]_2[Yb(C_8H_8)_2]$ shows planar parallel eclipsed [8]annulene rings sandwiching a centrosymmetric ytterbium. A potassium coordinated with dimethoxyethane is at the opposite side of each ring. Crystals of $[K(C_4H_{10}O_4)]_2[Yb(C_8H_8)_2]$ crystallize in the triclinic system of space group $P\bar{1}$ with a = 9.346 (4) Å, b = 9.775 (4) Å, c = 7.740 (4) Å, α = 91.72 (4)°, β = 109.16 (4)°, and γ = 86.22 (4)° at T = 23 °C.

Introduction

The organolanthanide complexes involving lanthanide(III) ions and the [8]annulene dianion[1] include complexes of the type $K[Ln(C_8H_8)_2]$,[2] $Ce_2(C_8H_8)_3$,[3] $[Ln(C_8H_8)(OC_4H_8)][Ln(C_8H_8)_2]$,[4] $[Ln(C_8H_8)Cl\cdot(OC_4H_8)]_2$,[5] $(C_8H_8)LnR(C_4H_8O)_x$,[6] $(C_8H_8)Ce(O\text{-}i\text{-}C_3H_7)_2Al(C_2H_5)_2$,[7] and $Ln(C_8H_8)(C_5H_5)$.[8] The determination of the structures of

† Dedicated to the memory of the late Professor Earl L. Muetterties, who shared the same birthdate as one of us.

(1) Controversy exists in naming sandwich organometallic actinide and lanthanide compounds of cyclooctatetraene dianion; [8]annulene dianion is chosen here because this name properly describes the delocalization of charge in the ligand and also emphasizes the formal oxidation state of the metal. See: Zalkin, A.; Templeton, D. H.; Luke, W. D.; Streitwieser, A., Jr. *Organometallics* **1982**, *1*, 618.

0276-7333/85/2304-0052$01.50/0